Journal of Hazardous Materials, 3 (1979) 91—106

KINETIC MODEL AND TESTS FOR RUNAWAY THERMALLY INITIATED STYRENE POLYMERIZATION

J.A. NORONHA, M.R. JUBA, H.M. LOW, W.E. PASCOE, E.J. SCHIFFHAUER and B.L. SIMPSON

Eastman Kodak Company, Rochester, New York 14650 (U.S.A.)

(Received September 29, 1978)

Summary

An iterative analysis is presented which permits the step-by-step computation of the reaction rates, conversions, temperatures, pressures, and other variables during the runaway stage of a thermally initiated styrene polymerization contained in a sealed reactor. The highlight of this analysis is a derivation for the reaction rate as a function of reactant temperature and conversion.

Based on a heat transfer analysis of some tests conducted at ambient temperatures ranging to 200°C, the iterative analysis predicted the observed reaction rates, pressures, rates of pressure rise, and temperatures within order-of-magnitude accuracies. We feel that this type of analysis may be extended to some other monomer-polymer systems.

Introduction

Several calculation methods have been proposed for sizing pressure-relief devices for nonreactive systems [1,2]. However, for the case of exothermic reactive systems, the few proposed methods [3,4,5] only provide a broad outline of this complex problem. Its complexity is due to the severe variations in the reaction rates, viscosity, temperature, pressure, and composition of the reaction mixture. One complicating aspect is the inadequate technical understanding of reaction kinetics under runaway conditions which is the subject of this paper.

Some semiempirical models [6,7] have been proposed to describe the kinetic mechanisms for runaway polymerizations. However, the tedious and expensive collection of the required experimental data for every system is prohibitive. Hence we developed a kinetic model for a thermally initiated styrene polymerization system, anticipating an easy extension of the model to other systems.

The kinetic model's estimates of the reaction rate, pressure, and temperature are within an order of magnitude of the experimental results.

Discussion on deviation of the polymerization rate equation

The polymerization rate equation (eqn. (1)) is based on a classical free radical polymerization mechanism (i.e., initiation, propagation, and termination of the polymer chains).

$$R_p = A_p \left(\frac{A_i}{A'_t}\right)^{1/2} \eta_{s,T}^{1/2} [m]^2 \exp\left[-\frac{(E_p + E_{d/2} - E_{t/2})}{(R)(T)}\right] \quad (1)$$

The following assumptions and theories are used in this derivation (see details in Appendix 1):

(1) The initiation rate has a second-order dependence on monomer concentration as suggested by Flory [8] instead of a third-order dependence as suggested by Hui and Hamielec [6].

(2) A quasi steady-state radical population exists.

(3) The chain termination rate varies inversely with the viscosity of the polymerization medium because of the Trommsdorff Effect (i.e., the reduction of the macroradical mobility with increasing reaction viscosity). This effect significantly influences reaction rate [6,9,10].

(4) The rate constants have an Arrhenius dependence on temperature [11].

(5) The solution viscosity is a function of the polymer concentration and molecular weight, and can be determined by the Hillyer and Leonard method [12].

(6) The chain transfer reaction proposed by Hui and Hamielic [6] and Olaj et al. [13] affects the molecular weight distribution but it does not affect the reaction rate.

Iterative analysis

Fig. 1 is a flow sheet showing some significant aspects of the iterative analysis. Each loop of this analysis is conducted at a specified solution temperature T°K. Some of the variables computed in each loop are: the monomer conversion (S), polymer concentration (C), monomer and polymer volume fractions, effective polymer molecular weight (M_{eff}), cumulative number average molecular weight ($\bar{M}_n$), cumulative weight average molecular weight ($\bar{M}_w$), solution viscosity ($\eta_{s,T}$), polymerization rate (R_p), ratio of polymerization rates between the current and previous steps (G), the total pressure (P_t), and the partial pressures of the monomer (P_m), the solvent (P_o), and the nitrogen (P_n).

Experimental system

To validate the kinetic model, we conducted a series of "statistically designed" experiments. The experimental system, shown in Fig. 2, is a modific tion of some isothermal calorimetric reactors commonly used to monitor reaction rates [14—17]. The principal modification of these experimental

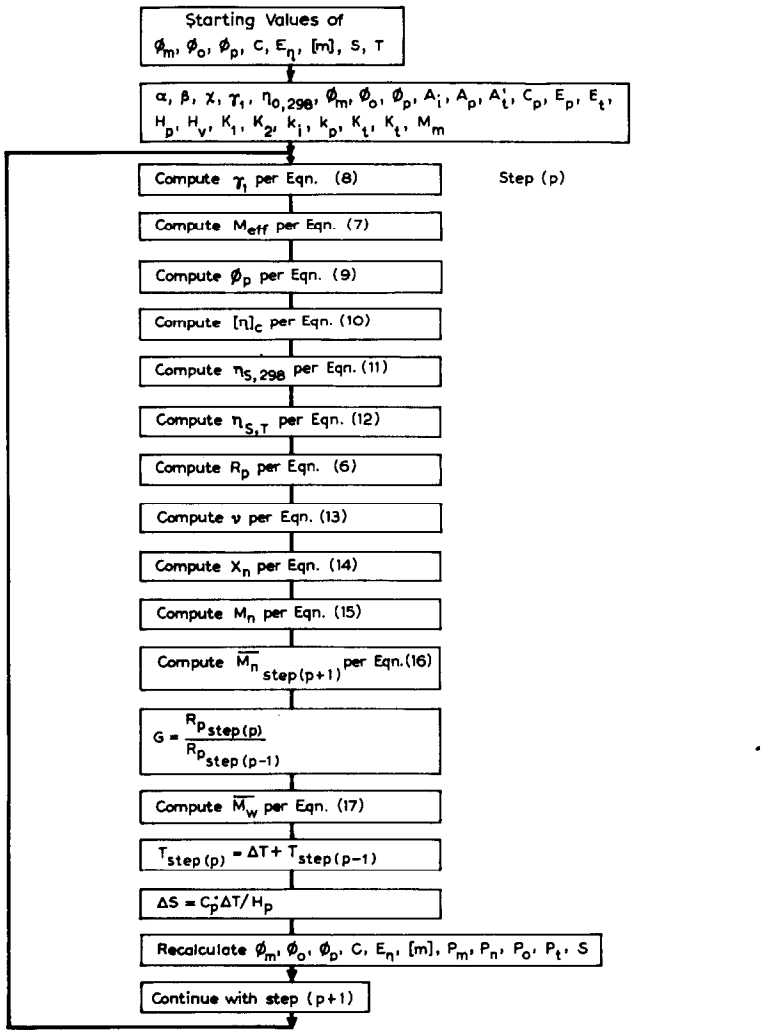

Fig. 1. Iterative analysis of an adiabatic thermally initiated styrene polymerization.

systems was to design an adiabatic reactor for high pressures. The reaction vessel is a 300-ml stainless steel pressure bomb equipped with three type-J thermocouples, a 180-ml glass liner, and a pressure gauge (0—140 psig). The experiments were conducted in a high-pressure bay and observed by closed-circuit television.

The reactant mixtures had an initial conversion of 0, 15, and 30 wt.% of a high-purity, high-molecular-weight polystyrene dissolved in styrene monomer. The monomer was purified by washing with dilute caustic and distilling under reduced pressure. In each test about 110 g of the initial polymer/monomer reactant solution was taken from 0°C storage. The reactor was then

sealed and the system was degassed by evacuating it five times to 710 mm Hg vacuum, holding the vacuum for about 2 min, and releasing it with oxygen-free nitrogen. An external electric heater controlled the ambient temperature and supplied the heat to initiate the reaction. Later, as the reaction rate increased, the reaction itself generated heat at a significantly higher rate than the heater input. This arbitrarily defined the runaway stage.

Experimental analysis

Pressure and temperature data for Test No. 9 are shown in Fig. 3. The ob-

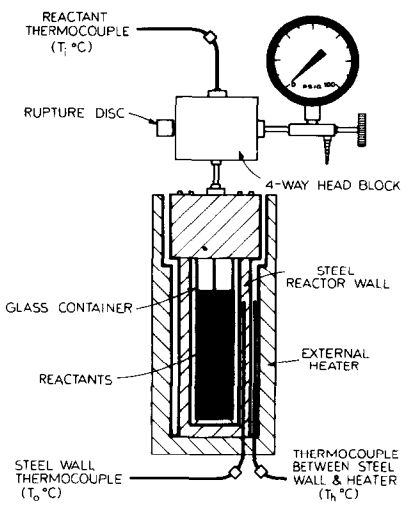

Fig. 2. Experimental setup.

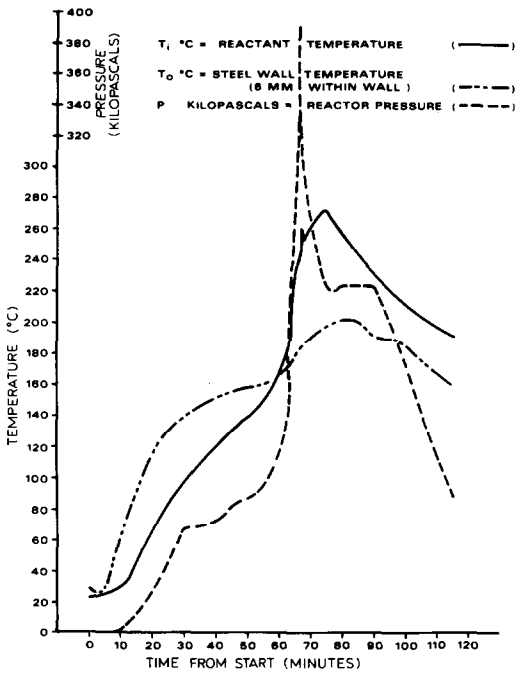

Fig. 3. Temperature and pressure data: Test 9.

served reactor pressure is the sum of the partial pressures of nitrogen and the styrene monomer which has vaporized from the reaction mixture. Note that the styrene's partial pressure cannot be greater than the styrene-polystyrene mixture's theoretical vapor pressure. The latter is an increasing function of temperature and a decreasing function of conversion. In our iterative analysis, the Flory—Huggins relationship [18] was used to compute the vapor pressures at the observed temperatures and the estimated conversions. Fig. 4 compares the observed and predicted temperatures and pressures for Test 6.

The computations to determine the experimental reaction rates are based

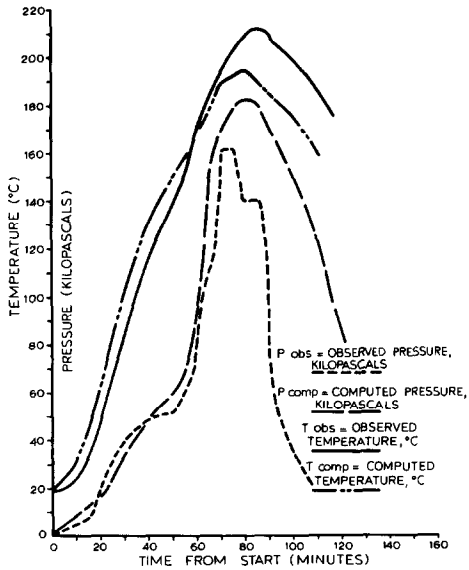

Fig. 4. Comparison of observed and predicted temperatures and pressures: Test 6.

on an unsteady-state heat-transfer analysis of the experimental system. Appendix 2 shows the computations for the overall heat transfer coefficient of the experimental system and the derivation of the formula used for the computation of the experimental reaction rates. Table 1 compares some reaction rate computations from this experimental analysis and the theoretical iterative analysis. Note that the iterative analysis applies only to an adiabatic reactor system, and hence the comparisons in Table 1 are made only during the runaway stage. The range of computed reaction rates shown in Table 1 is determined by the various solutions of the iterative analyses which approximately simulate the measured parameters (i.e., time, temperature and pressure). These solutions are obtained from different possible initial conditions at the onset of the runaway stage.

Sources of computational and experimental errors

The absence of agitation of the reaction medium introduced errors in the experiments because of the nonuniform solution temperature and the reduced sensitivity of the temperature sensor in the unagitated solution. These errors increased as the solution viscosity increased. A second source of error was the large ratio of reactor surface area to reactant volume in the small reactor. This caused significant heat losses during the runaway stage which were not accurately accounted for in our kinetic model. A third source of error was the neglecting of the contribution of the convective heat transfer in the nitrogen-styrene vapor gap to the overall heat transfer coefficient "U_0" (see Appendix 2)

TABLE 1

Comparison of computed reaction rates based on model with rates calculated from experimental temperatures. Tests 1, 5, 7, 9, 10, 11

Test No.	Initial degree of conversion (wt. %)	Observed reaction medium temp. T_i (°C)	Observed temp. 6 mm within reactor wall T_o (°C)	$(T_i - T_o)$ (°C)	$\frac{dT_i}{dt}$ (°C/min)	Expt. reaction rate based on eqn. (28) ($R_p \times 10^4$) (mole/l-s)	Range of reaction rates computed per model eqn. (1) ($R_p \times 10^4$) (mole/l-s)
2	0	130	151	−21	1.9	4.42	1— 2
		140	154	−14	1.9	6.05	3— 6
		150	155	− 5	2.4	11.21	8—11
		160	160	0	2.4	12.51	13—18
		170	167	+ 3	2.9	17.88	16—21
5	15	130	157	−27	2.3	4.67	3— 5
		140	158	−18	1.8	6.73	4— 9
		150	160	−10	1.7	5.96	8—11
		160	163	− 3	2.5	12.04	10—16
		170	167	+ 3	2.5	13.60	18—50
7	30	130	153	−23	2.0	4.30	8—12
		140	156	−16	2.4	8.37	15—20
		150	159	− 9	2.9	12.75	25—31
		160	160	0	4.5	23.29	30—51
		170	179	+ 9	3.8	17.40	35—57
9	0	130	156	−26	1.9	3.13	1— 2
		140	157	−17	1.9	5.46	3— 6
		150	160	−10	3.6	15.73	8—11
		160	162	− 2	4.3	21.79	13—18
		170	164	+ 6	5.6	30.05	16—21
10	15	130	168	−38	2.6	3.31	3— 5
		140	169	−29	5.3	9.49	4— 9
		150	171	−21	4.2	15.95	8—11
		160	172	−12	5.9	27.07	10—16
		170	171	− 1	5.9	19.92	18—50
11	30	130	166	−36	2.4	2.89	8—12
		140	170	−30	2.3	4.16	15—20
		150	167	−17	2.5	8.43	25—31
		160	166	− 6	5.3	25.45	30—51
		170	171	+ 1	7.1	36.38	35—57

Results

(1) The iterative analysis predicted the reactant temperatures and the reactor pressures during the adiabatic runaway stages of the tests with adequate accuracy for a reactor design. (The agreement between the experimental and predicted temperature and pressure values was about 10% in the best case and about 75% in the worst case.)

(2) The observed rates of reaction were of the same order of magnitude as predicted by the iterative analysis. This degree of accuracy was adequate in determining the order of magnitude of the rates of pressure rise.

(3) The maximum observed pressures were in the 200 to 350 kilopascals range. The observed rates of pressure rise were well below 700 kilopascals/s. This rate may be considered in the minimal hazard range for designing a venting system for this 300-ml reactor even though we are uncertain about the hydraulics of emergency venting. (Note that these tests were "contained" in the reactor. There was no intention to vent the reactor.)

(4) There was close agreement (15%) between the predicted and observed molecular weight distributions. However, an order of magnitude analysis indicates only a secondary dependence of the reaction rate on the molecular weight distribution. Consequently, we are investigating the possibility of obtaining an equivalent degree of accuracy by means of a simpler analytical analysis.

Limitations

(1) The temperatures and pressures developed were a function of the heat transfer characteristics of this reactor system. Hence, the observed pressures and temperatures related only to this system.

(2) The experiments were conducted at ambient temperatures up to 200°C. Hence, they would not relate to the high temperatures encountered if the reactor was exposed to an external fire.

(3) These results and the kinetic model applied only to runaway conditions of a thermally initiated polymerization of styrene. They should not be applied to the nonadiabatic stage of a reaction. In addition, they should not be applied to other polymerization systems without extreme care. For example, if a free radical initiator (i.e. peroxide or azo compound) were employed, the reaction rate and the rates of temperature and pressure rise could be considerably higher than indicated by the results of these experiments.

Thus while these experiments, coupled with other modeling efforts, could serve as useful guidelines, it would be difficult to develop generally applicable design criteria without carefully evaluating a broad range of monomer, polymer, initiator systems from a theoretical as well as an experimental standpoint.

Extension of the reaction kinetic equation to other polymerization systems

As the Trommsdorff effect is observed in nearly all free radical polymerizations with a high viscosity of the polymerizing medium, it would be interesting to extend this treatment to other polymerization systems. This could be done by replacing eqn. (5) (in Appendix 1) for the rate of initiation with a rate of initiation appropriate for another system. For example, the polymerization rate in eqn. (7) for a system employing a free radical initiator (i.e. a peroxide or azo compound) would be:

$$R_p = k_p\left(\frac{k_d f}{k'_t}\right)^{1/2} [I_2]^{1/2}\, \eta_{s,T}^{1/2}\, [m] \qquad (2)$$

For a copolymerization system eqn. (2) will not predict the impact of the Trommsdorff effect on the rate of polymerization. In such a case experimental values would have to be determined.

References

1 E. Jennet, Design considerations for pressure relieving systems, Chem. Eng., 67 (15) (Sept. 2, 1963) 83.
2 R.L. Salter, L.L. Fike and F.A. Hansen, How to size rupture discs, Hydrocarbon Process. Pet. Refiner, 42 (5) (May 1963) 159.
3 J.J. Boyle, Jr., Sizing relief area for polymerization reactors, Chem. Eng. Prog., 63 (8) (August 1967) 61.
4 J.E. Huff, Computer simulation of polymerizer pressure relief, AIChE Loss Prevention Series, CEP Technical Manual, 7 (1973) 45.
5 H.A. Duxbury, The Sizing of vents for gas flow and for polymerization reactors: A state-of-the-art review, Presentation at the Tenth Annual AIChE Loss Prevention Symposium, Kansas City, April 1976.
6 A.W. Hui and A.E. Hamielec, Thermal polymerization of styrene at high conversions and temperatures: An experimental study, J. Appl. Polym. Sci., 16 (1972) 749.
7 S.T. Balke and A.E. Hamielec, Bulk polymerization of methyl methacrylate, J. Appl. Polym. Sci., 17 (1973) 905.
8 P.J. Flory, Principles of Polymer Chemistry, Cornell University Press, Ithaca, New York, 8th Printing, 1971, p. 131.
9 P. Hayden and H. Melville, The kinetics of the polymerization of methyl methacrylate I: The bulk reaction calorimeter reactor, J. Polym. Sci., 43 (1960) 201.
10 V.D. Enal'ev and V.I. Melnichenko, Mathematical modeling of vinyl polymerizations, Depvoiyrf Fovumrny, Biniyi (1974) 19.
11 G. Odian, Principles of Polymerization, McGraw-Hill Book Co., New York, 1970, p. 243.
12 M.J. Hillyer and W.J. Leonard, Solvents Theory and Practice, in R.W. Tess (Ed.), Advances in Chemistry Series, American Chemical Society, Washington, D.C., 124, 1973, p. 31.
13 O.F. Olaj, H.F. Kauffmann, J.W. Breitenbach and H. Bieringer, The Diels—Alder Intermediate as a chain transfer agent in spontaneous styrene polymerization II: Evidence from the comparison of the chain length distribution of spontaneously initiated and photo-initiated polymers, J. Polym. Sci., Polym. Lett. Ed., 15 (1977) 229.
14 John R. Ebdon and Barry J. Hunt, Study of the free radical polymerization of styrene by differential scanning calorimetry, Anal. Chem., 45 (1973) 804.
15 H.M. Anderson, Isothermal kinetic calorimeter applied to emulsion polymerization, J. Polym. Sci., Part A, 4 (1966) 783.
16 K.E.J. Barrett and H.R. Thomas, Calorimetric method for the determination of rate of emulsion polymerization applied to methyl methacrylate, Br. Poly. J., 2 (1970) 45.
17 R.H. Biddulph and P.H. Plesch, A new versatile apparatus for measuring the rates of fast liquid phase reactions, Chem. Eng. (London) (Nov. 12, 1959) 1492.
18 Flory, op. cit., p. 522.
19 S.W. Benson and A.M. North, Simple dilatometric methods of determining the rate constants of chain reactions, J. Am. Chem. Soc., 81 (1959) 1339.
20 J.D. Ferry, Mechanical properties of substances of high molecular weight III: Viscosities of the system polystyrene-xylene, J. Am. Chem. Soc., 64 (1942) 1330.
21 Odian, op. cit., p. 205.
22 A.E. Hamielec, Polymer Reactor Engineering Course Notes, Chpt. 1, Part 1, McMaster University, Hamilton, Ontario, 1977, p. 43.
23 Flory, op. cit., p. 334.
24 Odian, op. cit., p. 263.
25 Balke and Hamielec, op. cit., p. 922.

Appendix 1: Discussion on derivation of the reaction kinetic equation

The Trommsdorff effect (the increase in reaction rate caused by the increase in viscosity of the reaction medium) in free radical polymerization is believed to result from the decrease in the rate constant for chain termination with increasing solution viscosity [19]. Since this often caused a dramatic autoacceleration in the rate of polymerization, it was important to predict the magnitude of this effect in terms of easily calculated or measured parameters.

Benson and North [19] studied the effect of viscosity on the rate of termination in the polymerizations of methyl methacrylate and n-butyl methacrylate. They found that, as a consequence of the Trommsdorff effect, the rate of chain termination varies inversely with the viscosity of the polymerization medium.

In any free radical polymerization, as in the case of styrene, the termination rate, R_t, is given as:

$$R_t = \frac{2k_t' [R^\cdot]^2}{\eta_{S,T}} \tag{3}$$

and the polymerization rate, R_p, is given as:

$$R_p = k_p[\mathrm{m}][R^\cdot] \tag{4}$$

For the case of the thermally initiated polymerization of styrene, the initiation rate, R_i, is given by Flory [8] as:

$$R_i = 2k_i[\mathrm{m}]^2 \tag{5}$$

The steady-state concentration of free radicals, $[R^\cdot]$, in eqn. (1) is determined from the quasi-steady-state assumption that the termination rate (eqn. (3)) is approximately equal to the initiation rate (eqn. (5)).

It follows that:

$$[R^\cdot] = (k_i/k_t')^{1/2} \eta_{S,T}^{1/2} [\mathrm{m}] \tag{6}$$

and,

$$R_p = k_p(k_i/k_t')^{1/2} \eta_{S,T}^{1/2} [\mathrm{m}]^2 \tag{7}$$

The polymerization rate, R_p, can be expressed as a function of temperature by using Arrhenius-type equations for the kinetic constants [11]. Substituting these Arrhenius functions in eqn. (7) gives eqn. (1) as follows:

$$R_p = A_p \left(\frac{A_i}{A_t'}\right)^{1/2} \eta_{S,T}^{1/2}[\mathrm{m}]^2 \exp\left[-\frac{(E_p + E_{d/2} - E_{t/2})}{(R)\,(T)}\right] \tag{1}$$

The solution viscosity, $\eta_{S,T}$, in eqn. (1) is a function of polymer concentration and solution temperature. It can be determined by the method of Hillyer and

Leonard [12] as shown by eqns. (8—11):

$$M_{eff} = \overline{M_w} \exp(\phi_m^{-\beta\gamma_1} - 1) \tag{8}$$

$$\gamma_1 = \exp(\phi_p - \chi\phi_p^2) \tag{9}$$

Note that,

$$\phi_p = 1 - \phi_m - \phi_o \tag{10}$$

$$[\eta]_c = K_1 M_{eff}^{\alpha} \tag{11}$$

$$\eta_{S,298} = \eta_{0,298} [1 + [\eta]_c C \exp(K_2[\eta]_c C)] \tag{12}$$

Ferry [21] has shown that the solution viscosity can be expressed as a function of temperature by eqn. (13) as follows:

$$\eta_{S,T} = \eta_{S,298} \exp\left[+\frac{E_\eta}{R}\left(\frac{1}{T} - \frac{1}{298}\right)\right] \tag{13}$$

The cumulative weight average molecular weight, $\overline{M_w}$, in eqn. (8) can be determined by eqns. (14—20). In developing the iterative analysis, it was vital to distinguish between the instantaneous average properties of the polymers being formed at a given conversion and the cumulative average properties of all the polymers formed up to that conversion.

The kinetic chain length, ν, of a polymer being formed is the average number of monomer molecules being polymerized per each radical which initiates a polymer chain. The kinetic chain length is related to the previously derived kinetic eqns. (1—4) as follows [22]:

$$\nu = \frac{k_p^2 [m]^2}{2k_t R_p} \tag{14}$$

For the homopolymerization of styrene, the predominant termination is achieved by the combination of two radicals. There is negligible chain transfer or termination by disproportionation. Hence, the instantaneous number average degree of polymerization, X_n, of the polymers being formed is given as follows:

$$X_n = 2\nu \tag{15}$$

The instantaneous number average molecular weight, M_n, of the polymers being formed is given as:

$$M_n = M_m X_n \tag{16}$$

Similarly, the cumulative number average molecular weight, $\overline{M_n}$, of all the polymers formed is given as:

$$\overline{M_n} = M_m \overline{X_n} \tag{17}$$

The physical meaning of the cumulative number average degree of polymerization, X_n, is:

$$\overline{X_n} \equiv \sum_{Z=1}^{\infty} \text{(actual chain length 'Z') (Number fraction of molecules of that actual chain length)} \quad (18)$$

This can be expressed mathematically as [23]:

$$\overline{X_n} = \sum_{Z=1}^{\infty} Z\,F(Z) \,/\, \sum_{Z=1}^{\infty} F(Z) \quad (19)$$

Eqns. (14), (15), and (16) compute ν, X_n, and M_n at each step of an iterative analysis. We can then compute $\overline{M_n}$ as follows:

$$\overline{M_{n_{step(p+1)}}} = \frac{(S)(\overline{M_{n_{step(p)}}}) + (\Delta S)(M_{n_{step(p)}})}{S + \Delta S} \quad (20)$$

where S = total monomer conversion before step (p) and ΔS = incremental conversion at step (p).

Flory [23] has shown that the cumulative weight average molecular weight is approximately twice the cumulative number average molecular weight for the most probable distribution. This distribution could be expected at low conversions where the magnitude of the Trommsdorff effect is small. However, Odian [24] claims that at higher conversions, when the Trommsdorff effect is large, the ratio of the cumulative weight to cumulative number average molecular weights shifts from 2 to 5. This is consistent with the results reported by Balke and Hamielec [25] for the bulk polymerization of methyl methacrylate, which has a large Trommsdorff effect. It is also confirmed by our measurements for the styrene system discussed in this paper. Hence, it follows:

$$\overline{M_w} = H\,\overline{M_n} \quad (21)$$

where $H = 2$ for the low Trommsdorff region and $H = 2$—5 for the high Trommsdorff region.

Appendix 2: Computations for the overall heat-treatment coefficient of the experimental setup and the reaction rate

Fig. 5 shows the heat transfer model of the experimental setup. Note that during the runaway stage, the radial heat transfer from the reactor is significantly higher than the heat transfer in the axial direction. This analysis assumes that the temperature of the reaction medium is uniform. At a given time, t, the unsteady-state heat-transfer rate, q, directed radially through the glass,

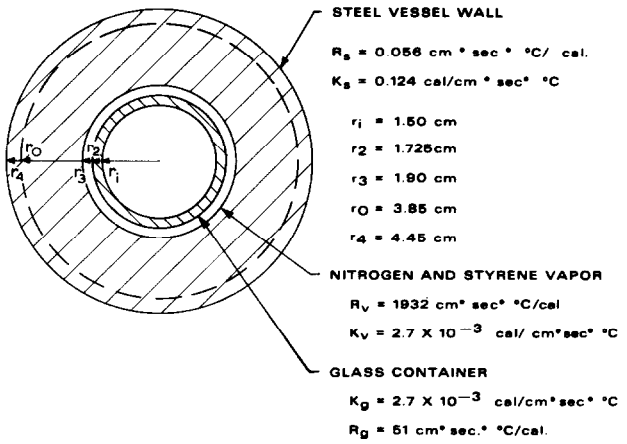

Fig. 5. Heat-transfer model.

vapor, and steel layers may be expressed as:

$$q = \frac{2\pi K_g(T_i - T_2)}{\ln(\frac{r_2}{r_i})} = \frac{2\pi K_v(T_2 - T_3)}{\ln(\frac{r_3}{r_2})} = \frac{2\pi K_s(T_3 - T_0)}{\ln(\frac{r_0}{r_3})} \tag{22}$$

Since only temperatures T_i and T_0 were measured, we rearranged these equations and expressed them in terms of R_g, R_s, R_v, and U_0, as follows:

$$q = \frac{2\pi\ (T_i - T_0)}{\frac{\ln(\frac{r_2}{r_i})}{K_g} + \frac{\ln(\frac{r_3}{r_2})}{K_v} + \frac{\ln(\frac{r_0}{r_3})}{K_s}}$$

$$= \frac{2\pi\ (T_i - T_0)}{R_g + R_v + R_s} \tag{23}$$

$$= U_0 A_0\ (T_i - T_0)$$

$$= 3.174 \times 10^{-3}\ (T_i - T_0) \tag{24}$$

Hence,

$$U_0 = 1.312 \times 10^{-4}\ \text{cal/cm}^2\ \text{s}\ ^\circ\text{C}. \tag{25}$$

The reaction rates during the runaway stages of the polymerization tests were computed from the temperature plots.

At a given time t min, the unsteady heat balance on the reaction medium may be expressed as:

$$\left(\frac{mc_p}{60}\right)\left(\frac{dT_i}{dt}\right) = H_p R_p V - U_0 A_0\ (T_i - T_0) - H_v E_v \tag{26}$$

The term $H_v E_v$ in eqn. (26) is negligibly small. Therefore, by rearranging eqn. (26) and solving for R_p, we have:

$$R_p = \frac{\left(\frac{mc_p}{60}\right)\left(\frac{dT_i}{dt}\right) + U_0 A_0 (T_i - T_0)}{H_p V} \tag{27}$$

and upon substitution of the appropriate values for the constants, eqn. (27) is simplified to the form:

$$R_p = 5.13 \times 10^{-4} \frac{dT_i}{dt} + 2.59 \times 10^{-5} (T_i - T_0) \tag{28}$$

Glossary of terms

α ≡ constant used in eqn. (11), dimensionless units,
= 0.5, for any system.

β ≡ constant used in eqn. (8), dimensionless units,
= 0.166, for polystyrene in styrene.

χ ≡ Flory–Huggins constant used in eqn. (9), dimensionless units,
= 0.4, for polystyrene in styrene.

ν ≡ kinetic chain length, dimensionless units.

γ_1 ≡ solvent activity coefficient, dimensionless units.

$[\eta]_c$ ≡ incremental change in relative viscosity, dl/g.

$\eta_{0,298}$ ≡ monomer viscosity at 298°K, cp,
= 0.6, for styrene.

$\eta_{S,298}$ ≡ solution viscosity at conversion 's' and temperature 298°K, cp.

$\eta_{S,T}$ ≡ solution viscosity at conversion 's' and temperature T°K, cp.

ϕ_m ≡ monomer volume fraction in solution, dimensionless.

ϕ_0 ≡ volume fraction of other components in solution, dimensionless units.

ϕ_p ≡ polymer volume fraction in solution, dimensionless units.

A_i ≡ frequency factor for monomer thermal decomposition l/mole s,
= 1×10^6, for styrene.

A_o ≡ area per unit length of cylindrical surface at radius r_0, cm.

A_p ≡ propagation frequency factor, l/mole s,
= 4.5×10^6, for styrene.

A'_t ≡ effective termination frequency factor, cp l/mole s,
= 3.5×10^7, for styrene.

C ≡ polymer concentration, g/dl.

C_p ≡ solution heat capacity, cal/g °C,
= 0.534, for styrene-polystyrene solution.

E_d ≡ activation energy for monomer thermal decomposition, kcal/mol,
= 25, for styrene.

E_p ≡ propagation activation energy, kcal/mole,
= 7.3, for styrene.

E_t ≡ termination activation energy, kcal/mole,
= 1.9, for styrene.

E_v ≡ vaporization rate for styrene monomer, g/s.

E_η ≡ activation energy for viscous flow of the solution, kcal/mole. (This is computed using a spline function based on tabular data.)

f ≡ initiator efficiency factor, dimensionless units.

$F(Z)$ ≡ distribution function of the number of molecules with an actual chain length 'Z', dimensionless units.

G ≡ ratio used in Fig. 1, dimensionless units.

I_2 ≡ initiator concentration, mole/l.

H_p ≡ heat of polymerization, cal/mole,
= 17.3×10^3, for styrene.

H_v ≡ heat of vaporization of monomer, cal/gram,
= 84.7, for styrene.

K_1 ≡ Mark–Houwink constant, dl/g,
= 2.5×10^{-3}, for polystyrene.

K_2 ≡ Martin viscosity coefficient, dimensionless units,
= 0.077, for styrene.

K_g ≡ glass container thermal conductivity, cal/cm s °C,
= 2.7×10^{-3}, for test container.

k_i ≡ initiator rate constant, l/mole s,
= 4.2×10^{-11}, for styrene at 100°C.

k_p ≡ propagation rate constant, l/mole s,
= 51.9, for styrene at 100°C.

K_s ≡ stainless steel reactor thermal conductivity, cal/cm s °C,
= 0.124, for the test vessel.

k_t ≡ termination rate constant, l/mole s,
= 10.5×10^6, for styrene at 100°C.

k'_t ≡ effective termination rate constant, cp l/mole s,
= 6.3×10^6, for styrene at 60°C.

K_v ≡ thermal conductivity of the monomer-nitrogen vapor mixture, cal/cm s °C.
= 9.9×10^{-2}, for styrene-nitrogen mixture.

m ≡ solution mass, g,
= 100—110, for these tests.

[m] ≡ monomer concentration, mole/l.

M_{eff} ≡ effective molecular weight, dimensionless units.

M_m ≡ monomer molecular weight, dimensionless units,
= 104, for styrene.

M_n ≡ instantaneous number average molecular weight of polymer being formed, dimensionless units.

$\overline{M}_n$ ≡ cumulative number average molecular weight of all polymers formed, dimensionless units.

$\overline{M}_w$ ≡ cumulative weight average molecular weight of all polymers formed, dimensionless units.

P ≡ observed reactor pressure, kilopascals (gauge).

P_m ≡ computed partial pressure of styrene, kilopascals (abs.)

P_n ≡ computed partial pressure of nitrogen, kilopascals (abs.).

P_o ≡ computed partial pressure of other solution components, kilopascals (abs.).

P_t ≡ computed reactor (total) pressure, kilopascals (gauge).

P_v ≡ computed pure styrene equilibrium vapor pressure at T_i °C, kilopascals (abs.).

q ≡ radial heat transfer rate per unit length of cylindrical surface, cal/s cm.

r_i, r_0, r_2, r_3, and r_4 ≡ see Fig. 5 in Appendix 1.

R ≡ Ideal Gas Law constant,
= 1.98 cal/mole °K.

$[R^{\cdot}]$ ≡ free radical steady state concentration, mole/l.

R_g ≡ thermal resistance of glass layer, cm s °C/cal.

R_i ≡ initiation rate of free radicals, mole/l s.

R_p ≡ polymerization rate, mole/l s.

R_s ≡ thermal resistance of steel layer, cm s °C/cal.

R_t ≡ termination rate, mole/l s.

R_v ≡ thermal resistance of vapor layer, cm s °C/cal.

S ≡ weight fraction of conversion, dimensionless units.

t ≡ time from start of experiment, min.

T ≡ solution temperature, °C.

T_i, T_0, T_2, T_3, and T_4 ≡ corresponding temperatures at radii r_i, r_0, r_2, r_3, and r_4 respectively, °C.

T_h ≡ observed temperature near heater, °C.

T_S ≡ heater temperature setting, °C.

U_0 ≡ overall heat-transfer coefficient of the section of the test system between radii r_i and r_0, cal/s cm^2.

V ≡ solution volume, l.

X_n ≡ instantaneous number degree of polymerization of polymers being formed, dimensionless units.

$\overline{X}_n$ ≡ cumulative number average degree of polymerization of all the polymers formed, dimensionless units.

Z ≡ actual chain length of a given polymer unit, dimensionless units.